JOURNAL OF GEOPHYSICAL RESEARCH, VOL. 103, NO. D10, PAGES 11,251–11,261, MAY 27, 1998

Changing lower stratospheric circulation: The role of ozone and greenhouse gases

Hans-F. Graf, Ingo Kirchner, and Judith Perlwitz

Max-Planck-Institut für Meteorologie, Hamburg, Germany

Abstract. Stratospheric climate has changed significantly during the last decades. The causes of these changes are discussed on the basis of two different general circulation model experiments forced by observed greenhouse gas and ozone concentration. There is a clear and significant response of the lower stratosphere temperature and geopotential in the model simulations forced by observed ozone changes that is in accord with observed trends in summer in middle and high latitudes of the northern hemisphere. Little effect is seen in the tropics. In spring there occur the strongest anomalies/trends in both hemispheres at polar latitudes; however, the model response is late by 1 to 2 months and is much weaker than the observed effects. The ozone-forced model in winter of both hemispheres produces slight warming or no change instead of the slight cooling observed. The effects of enhanced greenhouse gases as taken from a transient IPCC scenario AGCM run do enhance the cooling in high latitudes in spring, but the effect is much smaller than observed. Hence neither of the two forcings (reduced ozone and increased greenhouse gases) in the cold seasons is able to produce the recent stratospheric and tropospheric trend patterns alone. These trends clearly resemble a natural mode of variability both in the model and in the real world. This mode associates a strengthened polar night vortex with an enhanced North Atlantic oscillation. The excitation of this mode cannot yet be attributed to anthropogenic forcing.

1. Introduction

Recent discussion and search for climate signals of increased greenhouse gas concentration, tropospheric aerosols, and stratospheric ozone depletion [e.g., *Santer et al.*, 1996] have clearly shown that stratospheric cooling is part of the anthropogenic signal. The secular increase in greenhouse gases leads to tropospheric warming, which is amplified by water vapor [*Flohn et al.*, 1992]. This warming first is strongest in the free troposphere at low latitudes; it generates a higher tropopause and, consequently, a cooler lower stratosphere. This phenomenon is known as the "troposphere-stratosphere compensational effect." Anthropogenic sulfate aerosol preferably in northern midlatitudes modulates the temperature effects near the surface but is expected to have negligible impact on the stratospheric temperature. A changed vertical distribution of ozone with slight increase of the generally low values in the troposphere and dramatic decrease due to homogeneous and heterogeneous chemical reactions with anthropogenic chlorine in the lower stratosphere during the last 2 decades will superpose to the greenhouse effect. Generally, an enhancement of the anomaly pattern can be expected with more absorption of solar radiation in the troposphere leading to higher temperatures there. The reduced ozone mass in the lower stratosphere results in diminished solar absorption, smaller heating rates, and lower temperatures. Since the most dramatic ozone destruction takes place via heterogeneous reaction at polar stratospheric clouds (or at volcanic sulfate aerosols), a strong annual cycle will be developed in ozone concentration anomalies and, therefore, in the temperature trends.

Copyright 1998 by the American Geophysical Union.

Paper number 98JD00341
0148-0227/98/98JD-00341$09.00

In this paper we will study the question of to what extent the two effects (more greenhouse gases and less stratospheric ozone) do affect the stratospheric temperature. Further, we are interested in how much the ozone effects in the stratosphere can contribute to observed tropospheric climate changes. In a recent paper [*Graf et al.*, 1995] we have shown that the long-term tropospheric greenhouse gas effects can change stratospheric winter circulation in a way that can strengthen the ozone reduction in high northern latitudes in winter. Since there does not yet exist a coupled climate model with realistic stratospheric circulation and coupled ozone chemistry and transport, here we study the potential of prescribed ozone variations to change circulation in the Hamburg climate model ECHAM in all seasons. This sensitivity test excludes all feedback which could lead to nonlinear amplification or damping of the effects, but it helps to identify the order of magnitude of the effects and, to a certain degree, attributes the observed changes to one or another anthropogenic forcing.

A comparable general circulation model study was recently published by *Ramaswamy et al.* [1996], who used the Geophysical Fluid Dynamics Laboratory SKYHI model and also prescribed observed ozone changes. This model operates with comparably simple tropospheric physics (for example, fixed clouds). However, in a recent study *Stenchikov et al.* [1997] showed that ECHAM4 GCM is not very sensitive to the tropospheric conditions when forced with stratospheric aerosols. Thus we have the chance to compare the results of a high-resolution stratosphere (SKYHI, 40 levels up to 80 km) with a low-resolution stratosphere (ECHAM4, 19 levels up to 30 km) model. Another study [*Zhao et al.*, 1996] also used prescribed ozone anomalies to drive an atmospheric circulation model. However, in this case only the late winter was studied for ozone changes owing to depletion at sulfate aerosols from volcanic eruptions. Hence these results only in part are comparable with the present study.

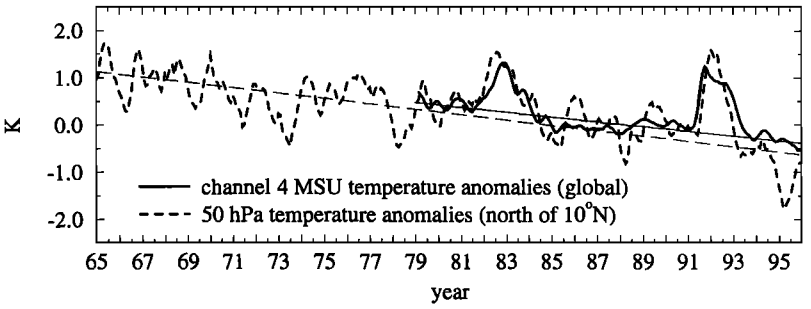

Figure 1. Global mean lower stratospheric temperature anomalies (in kelvins) derived from the MSU channel 4, which peaks near 70 hPa (solid line) and northern hemispheric mean 50-hPa temperature (north of 10°N) derived from radiosonde observations by the Stratospheric Group at the Free University of Berlin (dashed line). Anomalies are computed with respect to the 1984-1990 base period mean. The 5-month running averages are shown. The thin solid and dashed lines are the corresponding linear trends of the unsmoothed time series, if the 2 years after the eruptions of El Chichón (April 1982) and Mount Pinatubo (June 1991) are excluded. The trends are significant at least at the 99.9% level.

2. Observed Trends

2.1. Zonal Mean Trend Structures

For the estimate of observed temperature trends, we took observational data for the stratosphere from Microwave Sounding Unit (MSU) channel 4 as derived by *Christie* [1995] for the global lower stratosphere. These data are available from 1979 until now. Very clearly one can see in the global mean (Figure 1, solid line) that there exists a slight declining temperature trend, which is overlaid by a strong warming signal due to the absorption of near-infrared and terrestrial radiation by the sulfate aerosol, which is formed from the sulfur gas (H_2S and SO_2) injection into the stratosphere by the eruptions of the volcanos El Chichón (1982) and Mount Pinatubo (1991). A second, independent data set is available for the northern hemisphere only. It is routinely derived from radiosonde observations at the Free University of Berlin (FU) [*Pawson et al.*, 1993] for the levels 100, 50, 30, and 10 hPa. The northern hemisphere mean of these data is also shown for the 50-hPa level in Figure 1 (dashed line). The FU data show higher variability and also higher amplitudes in the volcanically disturbed years since, other than MSU data, they are not vertically smoothed and only represent the northern hemisphere. The linear trend function was computed after exclusion of the volcanic effect, that is, by omitting 24 months of data from the month of the eruption on. Both trends are statistically significant at least at the 99.9% level. This was tested using the unsmoothed data. The FU data also show a decline in lower stratospheric temperature.

In Figure 2 the zonal mean temperature trends in kelvins per decade for all months of the year are shown in terms of decadal linearized trends during January to June 1997 for the MSU data set (Figure 2a) and the new reanalysis data of the National Center for Environmental Prediction (NCEP; http://wesley.wwb.noaa.gov/reanalysis.html) and the National Center for Atmospheric Research (NCAR) for 50 hPa (Figure 2b).The trend analysis of observed zonal mean lower stratospheric temperature clearly shows the strongest effects at high latitudes in boreal and austral spring; these trends, however, only pass a statistical significance test (t test, chance of error <5%) in March and October, MSU only, respectively, because of the high variability of circulation and temperature in winter and spring in both hemispheres.

The MSU and the NCEP/NCAR trend structures can be compared with Figure 2b of *Ramaswamy et al.* [1996] and Figures 3a and 3b of *Labitzke and van Loon* [1995], respectively. While there is little difference for MSU and NCEP/NCAR, the FU trend pattern changed considerably, mainly in boreal midwinter, where *Labitzke and van Loon* [1995] found a rather strong warming in the north polar lower stratosphere. This warming is absent in our analysis, since we took off the effect of the volcanoes which led to low-latitude warming and polar cooling in winter. Since the Labitzke and van Loon analysis in the first years included the El Chichón effects, they find warming over the north pole in January, which is not compensated by Mount Pinatubo, since their time series ended just 1 month before this volcano erupted. Anyway, this warming was not of statistical significance; however, it clearly indicates the necessity for very careful analysis of different effects on stratospheric temperature. *Ramaswamy et al.* [1996] simply showed the difference in temperature between 1990 and 1979, thus circumventing the problem. Clearly, both independent data sets show similar structures of the northern hemisphere stratospheric temperature trends with amplified amplitudes in the NCEP/NCAR data. This is due to the vertical smoothing of the MSU data. Generally, in summer there is slight, but significant, cooling of the lower stratosphere from the subtropics to the pole. In winter, only the cooling at midlatitudes and in the subtropics is found, while at higher latitudes there are no significant trends. The exception is the month of March, which over northern polar latitudes in both data sets shows significant cooling by several centigrades per decade. This effect in spring is more pronounced in the northern hemisphere than over Antarctica, although there the reduction in ozone is much stronger. This indicates the probable impact of other effects.

In Figure 3 the observed trends in geopotential height of the 50-hPa layer are shown for the same years as in Figure 2. In this pattern in the northern hemisphere, two distinct and statistically significant (chance of error <1%) negative trends are found: one in spring north of the polar circle, and the other in summer and fall at the same place and reaching south in the subtropics. The amplitude in spring is larger with more than 350 geopotential meters (gpm)/10 years than the fall depression, which only reaches 100 gpm/10 years. We also found the same trend structure in FU data (not shown here). In the southern hemisphere, negative geopotential anomalies occur only during times when sunlight is available, which are strongest in November and December, that is, at the end of the Antarctic ozone hole season. This is an effect of reduced ozone and increasing solar radiation. The comparison of temperature and geopotential effects might suggest that the latter are due to

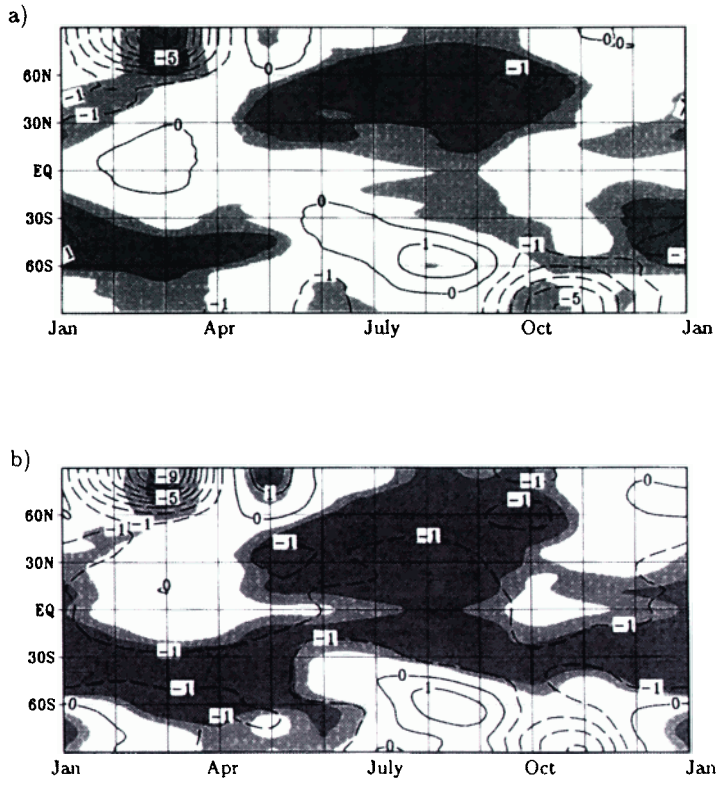

Figure 2. Observed zonal mean monthly temperature trends, January 1979 to June1997 (in kelvins per decade), of the lower stratosphere: (a) MSU channel 4 temperature and (b) 50 hPa temperature (NCEP data). Light (dark) shading indicates that the trends are significant at the 95% (99%) level of a local t test.

diabatic forcing, probably evoking from less absorption of solar radiation at the reduced ozone in the lower stratosphere. In winter the effects of diminished longwave irradiance and absorption counteract and give rise to negligible changes due to diabatic processes. This will be tested using a GCM simulation. The fact that the trends at high latitudes are stronger in the northern hemisphere, where the ozone trends are much smaller, indicates the importance of other mechanisms.

2.2 Trend Patterns

Graf et al. [1995] discussed 30-year trends of boreal winter circulation concerning their potential role in the process of chemical ozone destruction. Here we focus on the potential influence of ozone changes on circulation. Since the chemical destruction of stratospheric ozone probably did not start before 1979 or so, we have to concentrate now on shorter time-scales of less than 20 years. For such short trends the proof of statistical significance is much harder to get, and consequently there are no significant trend patterns found for the mean winter months December through February. At this time of year the variability is too high. The (not statistically significant) tendencies show cooling rather than warming in the lower stratosphere. The cooling tendency is consistent with the effect of higher greenhouse gas concentration as suggested by *Graf et al.* [1995].

The above picture changes clearly when geopotential and temperature of the lower stratosphere are investigated for March. For two independent data sets, the geopotential as derived from NCEP/NCAR and the microwave soundings from satellite [*Christie*,

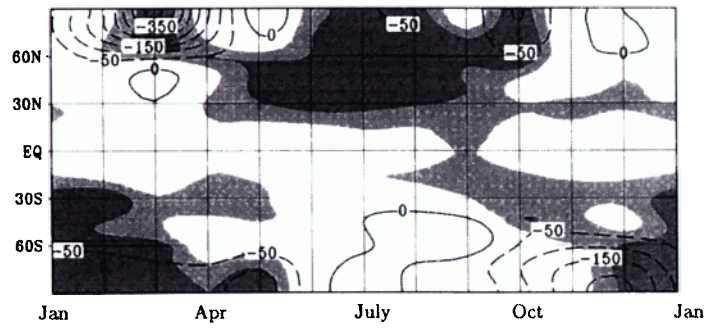

Figure 3. Observed zonal mean monthly 50-hPa geopotential trends, January 1979 to June 1997 (in gpm per decade) (NCEP data). Light (dark) shading indicates that the trends are significant at the 95% (99%) level of a local t test.

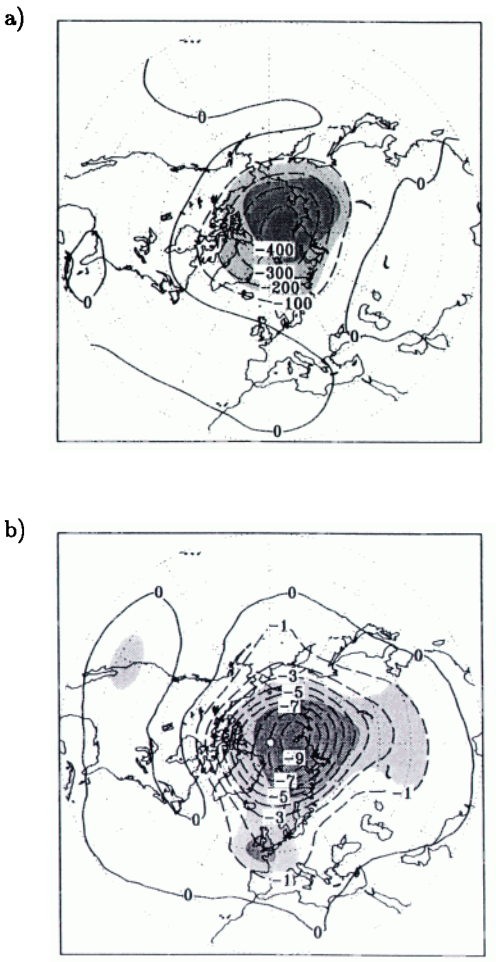

Figure 4. Observed northern hemispheric local linear trends, 1979-1997, in March for (a) 50-hPa geopotential height (in gpm per decade) (NCEP data) and (b) lower stratospheric temperature (MSU channel 4) (in kelvins per decade). Light (dark) shading indicates that the trends are significant at the 95% (99%) level of a local t test.

1995], which give the temperature of the lower stratosphere, coherent trend structures are shown in Figure 4. There is a strong decrease in the geopotential of the 50-hPa layer which reaches not less than 400 gpm per decade. This value goes along with a maximum of 9 K cooling per decade of the lower stratosphere. Both patterns are nicely centered at the pole with an only slight shift toward the Eurasian continent, suggesting that a possible process is the decreased radiative heating of the lower stratosphere due to less absorption of solar radiation at the reduced ozone after the polar night. This trend indicates a much stronger, more stable, and colder polar vortex in March. According to earlier investigations on the coupled modes of stratospheric-tropospheric circulation [*Perlwitz and Graf*, 1995], anomaly patterns in the troposphere should then be found with a stronger North Atlantic oscillation (NAO), warming over higher latitudes of Eurasia and cooling over Greenland and in the eastern Mediterranean. In Figure 5, these trend patterns, which are even statistically significant with 99% in the centers of the main anomalies, are found using NCEP/NCAR analyses of 500-hPa geopotential and MSU channel 2R temperatures. Since the association of enhanced stratospheric westerlies with a strong NAO depicts a coupled mode of atmospheric circulation, it remains unclear which one of the features is the leading one in our specific case. We will try to find an answer later with a GCM experiment. In the troposphere, in addition to the enhanced "baroclinic mode" [*Perlwitz and Graf*, 1995] also in the northern Pacific, significant trends appear which may have been induced by the increased equatorial sea surface temperature during the last decade. These trends indicate a southeastward shift of the Aleutian low. The positive lower tropospheric temperature trends over West Europe, central Siberia, and the west coast of North America are found at nearly the same positions as the positive geopotential trends, suggesting adiabatic warming due to sinking air at these places.

Figure 6 contains information about the temporal development of the stratospheric (Figure 6a) and tropospheric (Figure 6b) trend patterns. The curves were produced such that the observed trend patterns north of 20°N (Figures 4 and 5) were projected on the observed geopotential and temperature anomaly patterns of March of every year since 1979, including the years after El Chichón and Mount Pinatubo. Projection means the vector dot product between the observed trend data and the individual anomaly data after weighting with the geographical latitude. To facilitate the comparison of these time series, they were normalized by their standard derivations. Such projections clearly indicate the contribution of

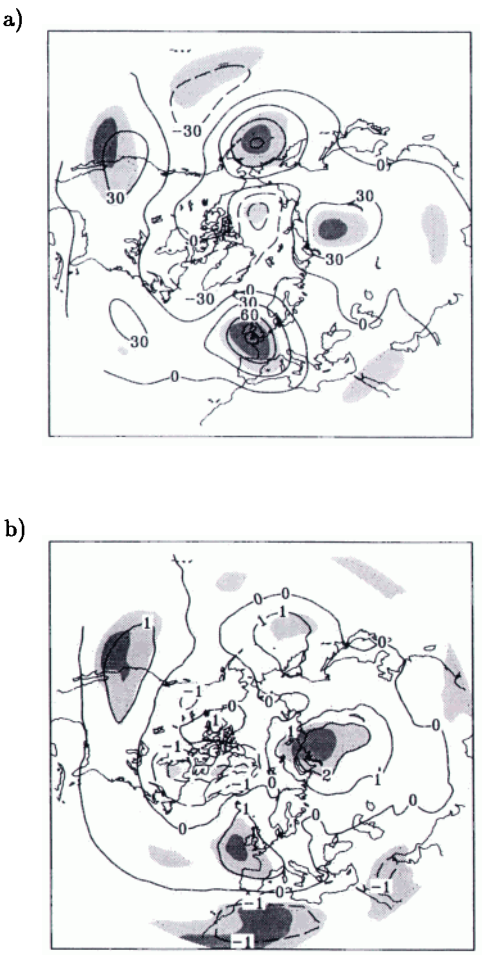

Figure 5. Observed northern hemispheric local linear trends, 1979-1997, in March for (a) 500-hPa geopotential height (NCEP data) (in gpm per decade) and (b) lower tropospheric temperature (MSU channel 2R, which peaks near 800 hPa) (in kelvins per decade). Light (dark) shading indicates that the trends are significant at the 95% (99%) level of a local t test.

individual years to the general trend pattern without having to inspect all individual patterns. Figure 6 shows the very strong correlation of the stratospheric and tropospheric parameters. With the exception of March 1989 and March 1997, a very close connection is also obvious between the tropospheric and the stratospheric patterns. This underlines the importance of coupled troposphere-stratosphere modes as discussed by *Perlwitz and Graf* [1995]. During the first decade, interannual variability is stronger than any possible trend, while after 1990 only smoothly increased values are seen. Possibly the effect of the stratospheric aerosol of the Mount Pinatubo eruption in 1991 stabilized the circulation by enhancing a natural circulation mode [*Graf et al.*, 1995]. The decadal trend patterns are therefore determined by the processes that took place only during recent years. Having this in mind, it is of interest to study the ozone abundance for the same years in order to make clear from what year spring ozone reduction took place in northern higher latitudes.

An inspection of the total ozone anomaly fields in March of the northern hemisphere since the beginning of the total ozone mapping spectrometer (TOMS) measurements in 1979 (not shown here) reveals two important insights: While during the first 10 years the variability of the ozone field was small (the maximum local anomalies hardly exceeded 40 Dobson units (DU)) and the deviation from the long-term mean (1979-1993) was generally positive, this changed from spring 1989 on. In March 1989 for the first time a -50 DU ozone anomaly appeared over northern Siberia which was embedded in a belt of reduced ozone at the midlatitudes of the northern hemisphere. From this year on the general pattern of ozone anomalies in spring was negative; that is, it indicated ozone loss over a large portion of the hemisphere. The maximum anomalies then were locally of the order of 80 to 100 DU and were strongest over northern Siberia. In order to facilitate the analysis, we computed the linearized trend pattern for ozone in March and projected this pattern (Figure 7a) on the individual ozone anomaly patterns of each March since 1979. The result is given in Figure 7b, showing that also the ozone trend pattern is accelerated by the evolution of recent years including the effects of the Mount Pinatubo eruption. This still leaves open whether any natural or anthropogenic circulation changes led to both, the temperature and ozone variations, or whether changed ozone itself played an active role for the observed features. To answer this question, we inspect the results of a GCM experiment which is forced by the observed ozone anomalies. A recent analysis of *Peters and Entzian* [1996] clearly indicates the dominating impact of changes in the tropospheric planetary waves on stratospheric ozone trends at midlatitudes for the winter months December through February. However, they did not analyze spring data yet.

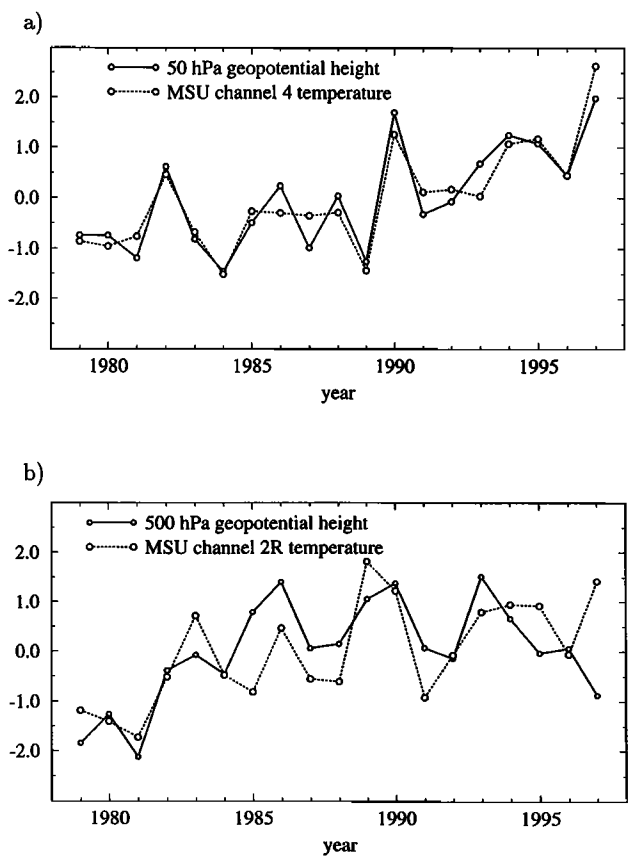

Figure 6. Normalized time series of the projection of March trend patterns to individual March anomaly patterns (a) for the northern hemispheric 50-hPa geopotential height (NCEP data) and channel 4 (lower stratosphere) MSU temperature and (b) for the northern hemispheric 500-hPa geopotential height (NCEP data) and channel 2R (lower troposphere) MSU temperature. The corresponding trend patterns are shown in Figure 4 and Figure 5.

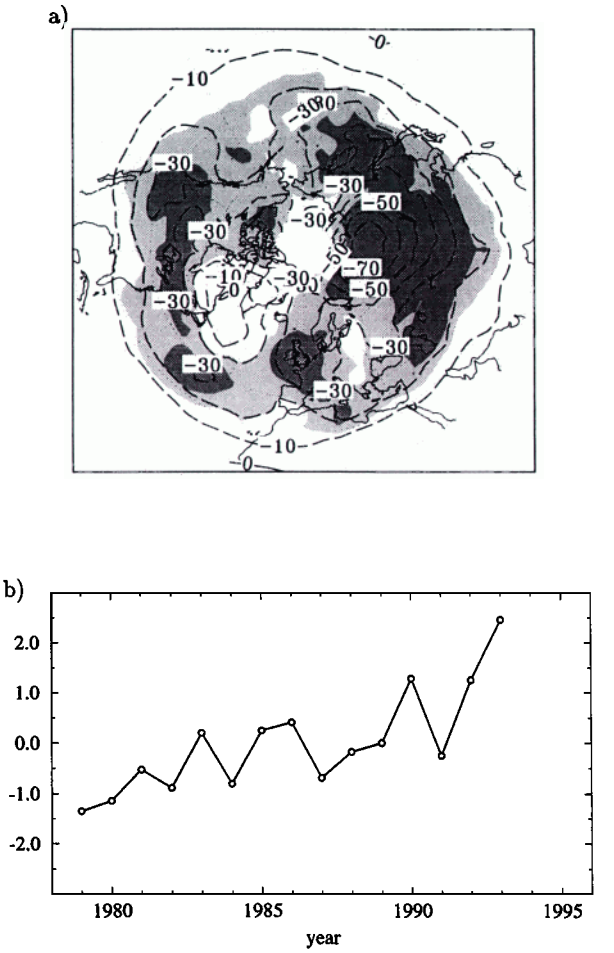

Figure 7. (a) Northern hemispheric local linear trends, 1979-1993, in March for total ozone (in DU per decade). Light (dark) shading indicates that the trends are significant at the 95% (99%) level of a local t test. (b) Normalized time series of the projection of the March trend pattern of Figure 7a to the individual March anomaly patterns.

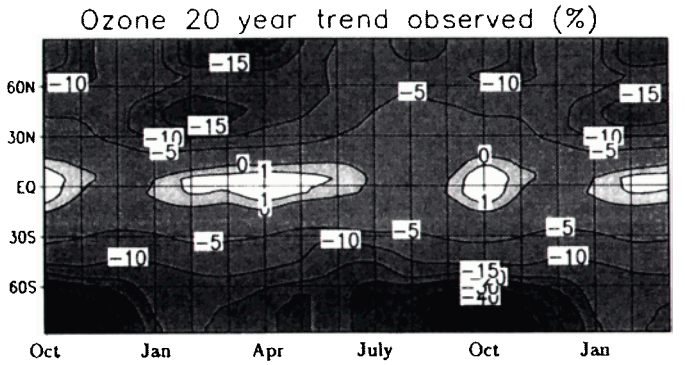

Figure 8. Ozone changes applied to the original ECHAM4 ozone field. Hovmöller diagram of zonal mean linearized 20-year trends based on data of *Herman et al.* [1993].

Comparison of the linearized ozone trends (Figure 7a) with temperature trends in the lower stratosphere (Figure 4b) shows remarkable similarity. The strongest ozone reduction is found right at the same place as the strongest cooling, over northern Siberia. The strong cooling of up to -9 K per decade enhances the chance of the formation of polar stratospheric clouds, which in a positive feedback loop lead to the destruction of ozone by heterogeneous chemistry. Probably there is also an impact of the weak significant increase of middle and upper tropospheric geopotential of more than 30 gpm per decade, over northern Siberia (Figure 5a). However, the positive anomaly of more than 60 gpm per decade has a much smaller effect on the stratospheric ozone over West Europe as well as over the Aleuteans, again indicating other than just planetary wave effects.

3. Model and Forcing

For our investigation we use the latest version of the Hamburg climate model ECHAM4. This model has been approved in many different studies, including the Atmospheric Model Intercomparison Project (AMIP) [*Gates*, 1992; *Stendel and Bengtsson*, 1996]. It is a 19-level T42 spectral model including state of the art standard physics. It was described in detail by *Roeckner et al.* [1992]. We did not couple the atmospheric model to an ocean model, but instead we used a prescribed sea surface temperature (SST) climatology for the years of the AMIP model intercomparison (1979-1988).

We took the ozone forcing from *Herman et al.* [1993], who used 13 years of Nimbus 7 TOMS, and derived zonal mean trends

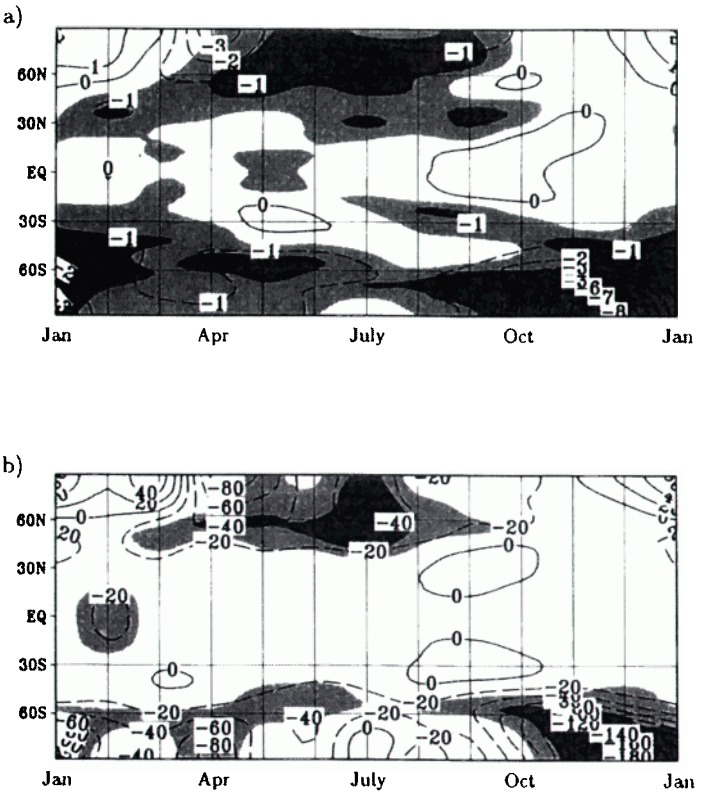

Figure 9. Response of the climate model to prescribed ozone from Figure 8 in the 70 hPa lower stratospheric (a) zonal mean temperature (anomalies in kelvins) and (b) zonal mean geopotential height (anomalies in gpm). Light (dark) shading indicates anomalies exceeding 1 (2) standard deviation(s).

of total ozone depending on latitude and month of the year after correction for solar cycle effects. The trend structure for zonal mean total ozone is given in a Hovmöller plot, latitude versus month of the year, in Figure 8. We used the original data from *Herman et al.* [1993] which are given in percent per decade and multiplied them by a factor of 2 in order to get a 20-year trend. These changes were then used to disturb the original ozone field of ECHAM [*London et al.*, 1976; *Wilcox and Belmont*, 1977]. This procedure implies that the linearized trends can be extrapolated, an assumption which is justified according to observations. Figure 8 makes clear that the strongest changes in ozone occur in southern polar regions in austral spring. This is the reflection of the strengthening of the Antarctic "ozone hole". The total ozone column over the south pole is less than 50% of the original value from September through November. Over the north pole the loss of ozone is less dramatic, reaching about 20% in April. A second maximum in ozone reduction is found at midlatitudes of the northern hemisphere in late winter. Its origin was suggested to be due to dynamics [*Graf et al.*, 1995] and to dynamics and chemistry [*Callis et al.*, 1997]. In the tropics there is very little or no change in total ozone, while throughout the year of the order of 10% less ozone is used as forcing of the climate model at higher latitudes.

For the equilibrium experiment the model was run for 11 years with the ozone forcing. This is prescribed on the T42 grid by linear interpolation of the original 5° resolution data to the 2.8° model resolution. Also the temporal resolution was interpolated to daily values from monthly means in order to avoid a stepwise forcing function. The first year of the experiment run is not analyzed for reasons of spinup. Thus we have 10 years of experimental data available.

The model's temperature response to the prescribed stratospheric ozone variation that was derived from observed trends (Figure 8) and extrapolated linearily to 20 years is given in Figure 9a. The patterns of the observed trends correspond very well with the response of the model to prescribed ozone changes. The main features are the cooling effects in austral and boreal spring which are due to less solar absorption. However, in the model calculations the northern hemisphere cooling in spring corresponding to the prescribed ozone forcing is shifted from March to April. This, as will be discussed later, may have a distinct impact on the troposphere response to the ozone forcing. In midwinter there is a diabatic warming tendency (rather than the cooling that was found for longer-term trends by *Graf et al.* [1995]) which, however, is not statistically significant owing to high variability. In the observations of Figures 2a and 2b this warming tendency is also not seen. It is probably overcompensated by another effect, namely, the strengthening of the midwinter polar vortex by increased greenhouse gas concentration in the atmosphere [*Graf et al.*, 1995]. This leads to increased geopotential heights at lower latitudes and thus to an enhanced polar night vortex with lower temperature inside the vortex. Hence short-term changes in stratospheric ozone recently superpose to the longer-term greenhouse gas effects.

The ozone-forced model shows a very weak general decrease of the 70-hPa geopotential (Figure 9b) and two stronger negative anomalies at very high latitudes in spring (i.e., April and May in the northern hemisphere and November and December in the southern hemisphere, respectively). The negative anomalies start with the reappearance of the Sun after polar night. As in the observations, the simulated temperature and geopotential anomaly and trend patterns correspond very well, indicating a direct thermal forcing of the stratospheric circulation by less absorption of solar radiation at the reduced ozone, a process which becomes more important when the Sun is at higher angles. The temporal delay of the simulated maximum negative temperature and geopotential anomalies in spring is suggested to be due to the missing effect of the enhanced baroclinic mode, as was discussed above. In our model simulation, only the diabatic effects of ozone are included, while the extra effects of increased greenhouse gases are missing. The anomalies in the southern hemisphere are much stronger, indicating an intensified south polar vortex in austral spring, during the season of the Antarctic ozone hole.

The geographical pattern of the model response to the observed ozone depletion is shown in Figure 10 for the northern hemisphere. Lower stratospheric temperature at high latitudes (Figure 10, left column) increases during the polar night by up to 4 K. Owing to high variability this anomaly is not statistically significant. It is most probably produced by inherent dynamic effects. Diabatic effects at the reduced ozone in polar latitudes during polar night are expected to be much weaker because of the counteracting

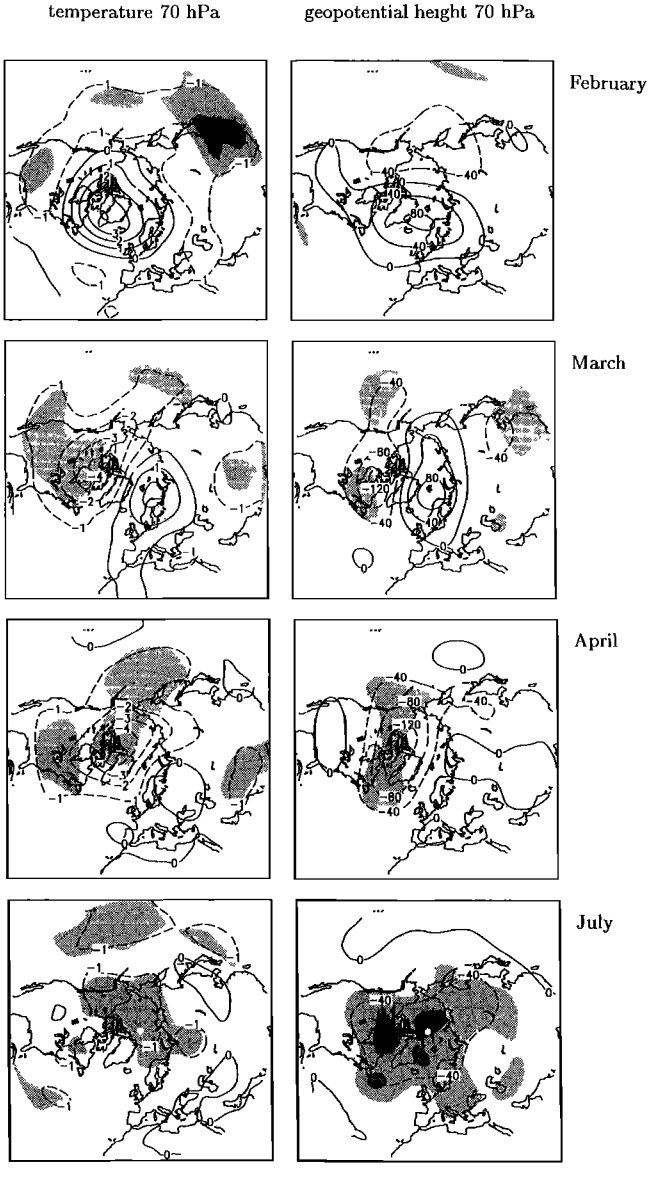

Figure 10. Polar stereographic projection of the climate model's response in 70-hPa temperature (left column, anomalies in kelvins) and geopotential height (right column, anomalies in gpm) for individual months.

reduced irradiance and absorption of infrared radiation, while the lower-latitude stratosphere is cooling owing to the stronger effect of less absorption of solar radiation at the depleted ozone layer. The geopotential height of the model 70-hPa layer increases by about 80 gpm at polar latitudes (Figure 10, right column), although this change is of as little statistical significance as the above mentioned temperature changes. The local anomalies reach at most 1 standard deviation of the model control run. Beginning in March, cooling occurs in the northern polar region in the lower stratosphere. However, this cooling is not as zonally symmetric as that in the observations, but instead it obtains a zonal wave number one structure with, in part, significant cooling over North America and warming still over northern Eurasia. This is opposite to the observations. In April the cooling becomes more centered over the pole and is then also visible in the zonal means (Figure 9). The analysis of patterns of the relative topographies 30 over 70 hPa (not shown here) clearly indicated that the April and later anomalies are due to internal stratospheric processes, that is, to local diabatic heating and cooling, while before April dynamic processes dominate.

In the model troposphere (not shown here) there is only minor response to the prescribed ozone change. Although the temperature and geopotential anomalies at some places exceed 1 and sometimes 2 standard deviations of the control run, the patterns are quite patchy and not stable over more than a period of 1 month. Even if one could accept any local significance of the computed anomalies, the global significance, which also has to take into consideration the spatial correlation of the variables, never reached an acceptable level of, for example, a 10% chance of error. Thus as opposed to the observations, in the model simulations we did not find the strengthening of the NAO pattern. One of the reasons for the failure of the simulation to resemble the coupled stratosphere-troposphere response, which is well pronounced in the observed data and was discussed above (Figures 4 and 5), may be the late cooling of the polar area. This possibly is caused by the too strong increase of temperature in winter as compared with the observed tendency. The delayed cooling of the polar stratosphere prevents the polar vortex from being forced above the critical zonal wind speed which could allow an impact on the tropospheric planetary waves. The background strength of the vortex is already too low in April to reach the limit. A second contribution to the failure may be that we have used zonal mean ozone changes and applied them to the model background ozone distribution. However, the observed ozone trends are strongly longitude dependent (Figure 7a). Thus probably the displacement of the main forcing as compared with observations also contributed to the differences between model and observation. Finally, of course, it is still possible that what we observe is simply a random effect of atmospheric circulation, and there is still the secular greenhouse effect which has to be considered here. In our model experiment we did not include the significant changes due to greenhouse gas forcing. As was already suggested by *Graf et al.* [1995], this type of forced anomalies over long times may have a stronger impact on stratospheric circulation and climate than do the ozone changes. They possibly only modulate the basic features of the anthropogenic greenhouse gas forcing.

As was already mentioned above, a clear difference exists in the timing of the northern hemisphere spring negative temperature and geopotential anomaly at polar latitudes. This anomaly in observations occurs already in March, while the ozone anomaly forcing produces the cooling only in April and May. The reason for this could possibly be the additional forcing by greenhouse gases. Therefore we investigated the trends of the CO_2-forced model from *Hasselmann et al.* [1995], who coupled the earlier climate model version ECHAM3 to a large-scale geostrophic ocean model and forced it with observed CO_2 concentrations. We studied the stability of zonal mean trend patterns in the course of the year for different 20-year periods starting in the mid-1960s and later in the transient CO_2 model experiment [*Hasselmann et al.*, 1995]. It became clear (without showing the figures here) that the linearized trends of geopotential are stable with time only at low latitudes, while at higher latitudes the strong variability of the trend patterns dominates. The increase of geopotential height at low latitudes supports the enhancement of the wintertime polar vortex. However, the variability at high latitudes with trend amplitudes of magnitude ±100 gpm per 20 years strongly modifies the dynamics. In the transient CO_2 experiment the negative trends of geopotential height of the 50-hPa level evolve slowly at north polar latitudes in fall. The amplitude of this anomaly is reduced and reaches with 140 gpm per 20 years only about 50% of the value which was observed for the years 1979-1997 (Figure 3). In April the model shows another negative trend, which is, however, not statistically significant. In March the CO_2 model experiment just like the ozone experiment shows minor tendencies. This is in clear contradiction to the observed behavior.

In Figure 11b the modeled time series of the relative winter DJF topography 300/700 hPa, indicating the heat content of the middle troposphere, and the relative topography 30/70 hPa (Figure

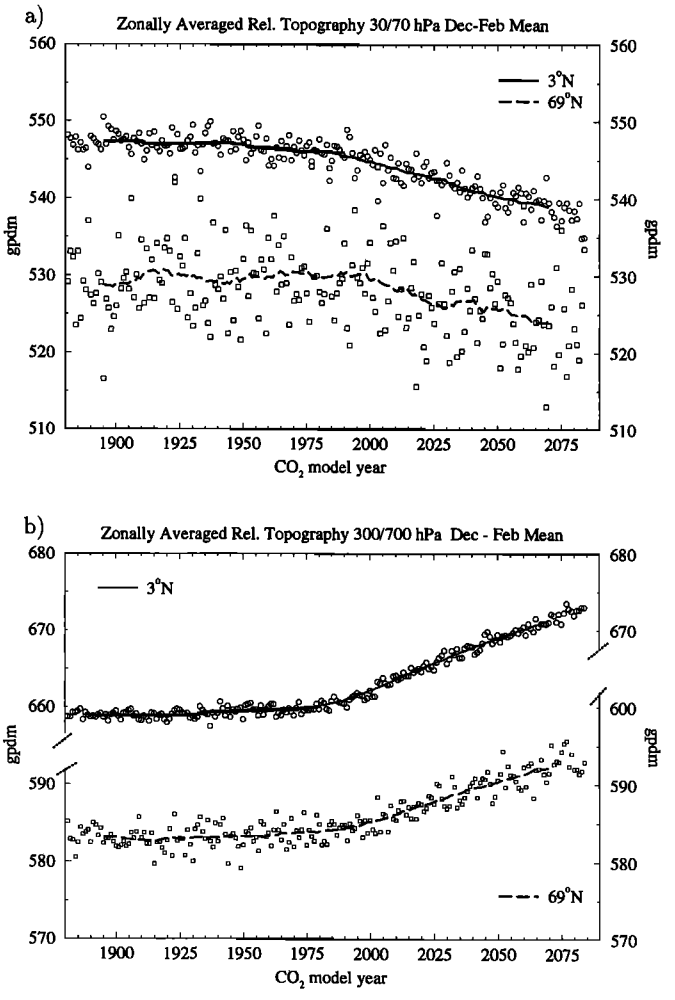

Figure 11. Relative topographies (a) 30/70 hPa and (b) 300/700 hPa (in geopotential decameters, gpdm) at 69°N and 3°N as modeled with ECHAM3/LSG for the transient increase of greenhouse gas concentration in the atmosphere (IPCC scenario A).

11a) as a measure of lower stratospheric heat content is given for 69°N latitude and for 3°N. Clearly, the warming of the polar and of the tropical troposphere is seen from the middle of the century on, while at the same time the tropical stratosphere cools in the winter months. Such variations may be due to natural model variability or to anthropogenic forcing. In the stratosphere the relative topography of the 700-year unforced control run, representing pure natural variability, at high latitudes seems to be influenced by a 50- to 60-year oscillation [*Perlwitz et al.*, 1996]. A weak remainder of this oscillation also exists in the tropics, where it is out of phase with high latitudes. The amplitude of the oscillation is with 40 gpm at the same order of magnitude as the expected greenhouse gas effect near the north pole, but it is much smaller in the tropical stratosphere. It is unclear so far whether or not this oscillation also influences the natural climate system and thus the timing of any climate signal forced by anthropogenic activity. Any clear negative trends of the polar lower stratospheric temperature do not appear before the model CO_2 year 2000 (Figure 11a). In the troposphere the modeled greenhouse gas induced trends start first at the low latitudes (Figure 11b), where the amplitudes of the changes are also larger than those at high latitudes. In the stratosphere the low latitudes nicely follow the compensational principle, while close to the northern pole the stratospheric cooling is delayed until the end of the model's 20th century. Any increase in lower stratosphere geopotential therefore is due to the tropospheric effects that are not compensated by stratospheric cooling.

At the end of boreal winter, in March, the tropospheric behavior to greenhouse gas forcing does not differ from the other winter months. In Figure 12 a Hovmöller diagram is given for the zonal mean relative topography 30/70 hPa for all northern latitudes in March. Here the decrease in heat content of the lower tropical stratosphere is seen as well as the erosion of the midlatitude "warm belt" that was discussed by *Graf et al.* [1995] as the result of planetary wave energy being dissipated at the edge of the northern polar night vortex.

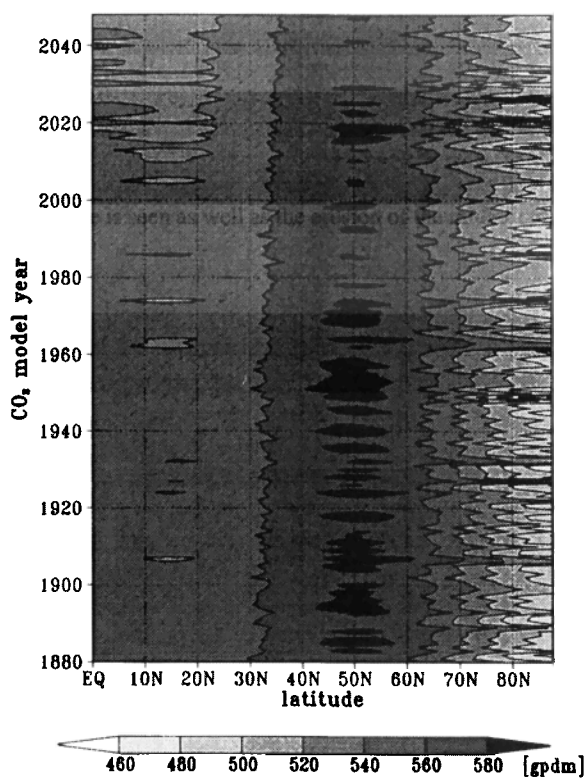

Figure 12. Hovmöller plot of zonal mean relative topography 30/70 hPa {in gpdm) for all northern latitudes.

On the basis of such short-term trends as 20 years, which is characteristic for the recent observed changes in stratospheric ozone, it is not possible to determine the physical reasons for the observed changes in atmospheric temperature and circulation with reasonable accuracy. It is well possible in the transient CO_2 experiment to find a 20-year trend that fits the observations well. Coincidentally, it is the model CO_2 years 1974 to 1993 which give this structure in the northern hemisphere (not in the southern hemisphere, and with a much smaller amplitude) that might misleadingly be used to "explain" the observations (Figure 13a). However, if we use trends that start 5 or 10 years later, the picture looks very different at high latitudes (Figures 13b and 13c). Hence the relatively weak, decadal forcing of combined greenhouse gases is not suited to serve as cause for the observed recent anomalies. In timescales of 20 years the atmosphere variability is still too strong, and at high latitudes the trends do not stably pass the significance limits. Only for longer trends (30 or 40 years, as in the work of *Graf et al.* [1995]) can the secular greenhouse gas effects be found with statistical significance and help explain the long-term atmospheric behavior. For shorter timescales, both ozone and greenhouse gas changes do not exert a strong enough forcing to successfully compete with natural variability.

4. Conclusions

Recent observations after elimination of volcanic effects show a global mean decreasing lower stratospheric temperature which is consistent with increased greenhouse gas scenarios. In winter at high latitudes this trend is less well documented, while the strongest trends occur in spring at high latitudes of both hemispheres. Since at this time also the stratospheric ozone concentration changes strongly, it was suggested [*Ramaswamy et al.*, 1996] that the anthropogenically reduced ozone is responsible for at least part of the observed temperature and circulation anomalies at high latitudes. We tested this hypothesis by forcing a sophisticated GCM with the observed monthly ozone changes and compared the resulting zonal mean anomalies as well as global patterns with observations of geopotential and temperature of the lower stratosphere. As did *Ramaswamy et al.* [1996], we found significant high-latitude cooling in spring of the northern hemisphere which is shifted from March to April in the northern hemisphere (from October to November in the southern hemisphere) when compared with observations. While this temporal shift was not discussed in detail by *Ramaswamy et al.* [1996], we think it is of some importance.

In addition, we studied the results of a transient greenhouse gas scenario experiment. The analysis of observed time series of stratospheric temperature and geopotential heights, as well as of the same parameters from GCM experiments forced with increasing greenhouse gas concentration, clearly shows that at higher latitudes of the northern hemisphere trends over only 2 decades are determined by natural variability rather than by the comparatively weak anthropogenic forcing.

The statistically significant observed trend patterns with strongly enhanced North Atlantic oscillation in March cannot be reproduced by forcing the GCM with observed ozone changes. Anomalies quite similar to the observed March trends do not appear in the forced models before April. Therefore we suggest interpreting the observed March anomalies as the result of dynamic changes in the troposphere, which may be due to natural variability or greenhouse gas forcing.

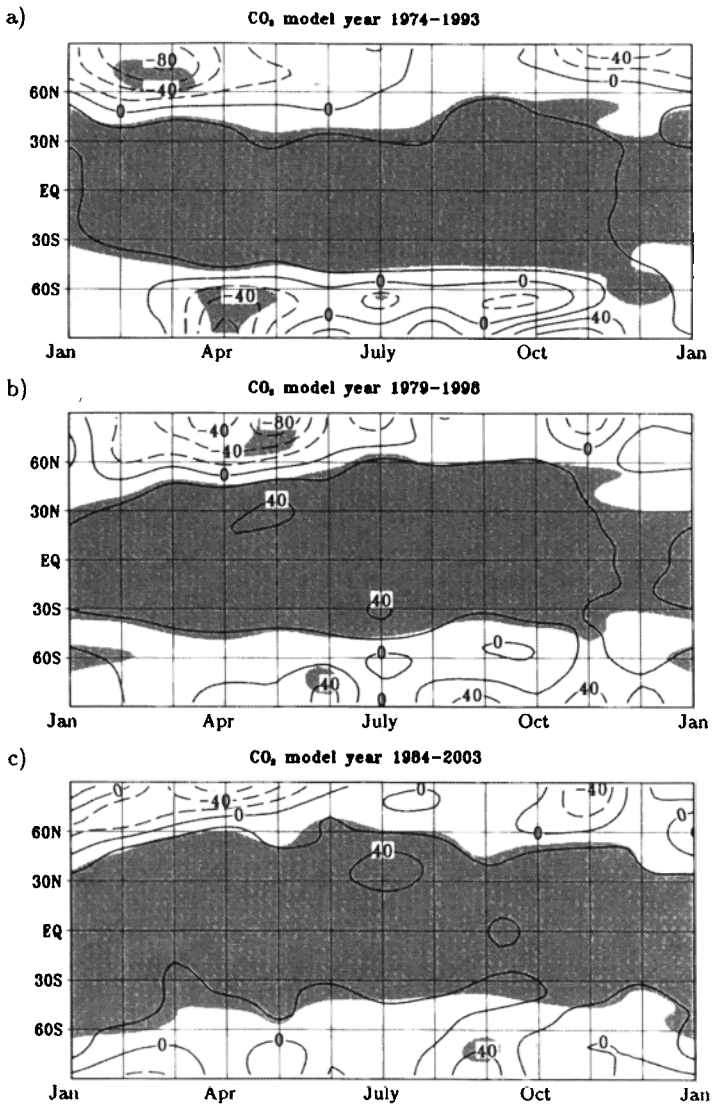

Figure 13. Linearized zonal mean monthly 20-year trends of the 70-hPa geopotential height (in gpm per decade) as modeled with ECHAM3/LSG for the transient increase of greenhouse gas concentration in the atmosphere (IPCC scenario A). Shading indicates that the trends are significant at the 95% level of a local t test. CO_2 model years: (a) 1974-1993, (b) 1979-1998, and (c) 1984-2003.

From the above discussed results we suggest that the observed polar symmetric cooling in boreal spring and strengthening of the polar vortex are not due exclusively to changed ozone nor exclusively to the greenhouse effect but, instead, possibly to a combined effect of both, ozone depletion and greenhouse gas forcing. Each forcing alone is much too weak to explain the observed features. In the model world in March the changed ozone content leads to cooling only over the polar western hemisphere, while the greenhouse forcing produces a more zonally symmetric enhanced polar vortex only in winter. We propose that the observed stratospheric circulation and temperature changes can be explained best by an initial enhancement of the north polar stratospheric vortex in early winter and midwinter due to lifting of geopotential layers at low latitudes by the combined greenhouse effect. At this point stronger evaporation from the sea surface and higher water vapor content of the troposphere will play the leading role. Alternatively, inherent long-period natural variability is a candidate for the quasi-stable enhancement of one of the leading atmospheric modes, the coupled NAO-polar vortex mode as is indicated by the low-frequency variability of the control run. The enhanced vortex increases the chances to be more closed off and to be less disturbed by vertically propagating planetary wave energy. Thus the quasi-stable mode of strong polar stratospheric vortex and enhanced North Atlantic oscillation is more probable than the opposite. Inside the cut off vortex the temperature decreases toward the radiative equilibrium, finally reaching temperatures that are supportive for polar stratospheric cloud and succeeding heterogeneous ozone destruction after sunrise. This sequence results in stronger cooling and a more stable vortex in spring, that is, in March and April. During the polar night reduced ozone slightly reduces the radiative cooling of the polar stratosphere, thus slightly counteracting the effects of greenhouse gases. In spring, however, reduced ozone and increased greenhouse gases both act in the same direction, strengthening and stabilizing the polar vortex.

Owing to the limited observations and the incomplete treatment of relevant physics and chemistry in the climate models, it is not yet possible to attribute the observed troposphere and stratosphere trends to one or another anthropogenic forcing. Rather we

can give some insight into some relevant processes. We find that for both simulations, the forced and the unforced, the basic process is the enhanced North Atlantic oscillation, which is coupled to a strong polar vortex in the stratosphere in the cold season. This dynamically enhanced vortex further is responsible for ozone depletion via heterogeneous reactions and changed transport and finally produces what is observed later in April. At this time, having just one realization of nature, we cannot decide what is the ultimate reason for the observed changes. We can only get a deeper insight in the process of the coupling between NAO and stratospheric winter vortex which is crucial in both cases. There is need to have further model simulations with variable ozone, and for such simulations it is essential to start the forcing at the right phase of low-frequency internal variability of the model.

Acknowledgments. We wish to thank Gera Stenchikov and an anonymous reviewer for their constructive comments. This work was supported by BMBF under a grant from Ozonforschungsprogramm.

References

Callis, L. B., M. Natarajan, J. D. Lambeth, and R. E. Boughner, On the origin of midlatitude ozone changes: Data analysis and simulations for 1979-1993, *J. Geophys. Res.*, *102*(D1), 1215-1228, 1997.

Christie, J. R ,Temperature above the surface layer, *Clim. Change, 31*, 455-474, 1995.

Flohn, H., A. Kapalan, H.-R. Knoche, and H. Mächel, Water vapour as an amplifier of the greenhouse effect: New aspects, *Meteorol. Z.*, *1*, 122-138, 1992.

Gates, W. L., The atmosphere model intercomparison project, *Bull. Am Meteorol. Soc.*, *73*, 1862-1870, 1992.

Graf, H.-F., J. Perlwitz, I. Kirchner, and I. Schult, Recent northern winter climate trends, ozone changes and increased greenhouse gas forcing, *Contrib. Phys. Atmos.*, *68*, 233-248, 1995.

Hasselmann, K., L. Bengtsson, U. Cubasch, G. C. Hegerl, H. Rohde, E. Roeckner, H. von Storch, R. Voss, and J. Waszkewitz, Detection of anthropogenic climate change using a fingerprint method, in *Modern Dynamical Meteorology: Proceedings from a Symposium in honour of Aksel Wiin-Nielsen*, edited by P. Ditlevsen, pp. 203-221, ECMWF Press, 1995.

Herman, J. R., R. McPeters, and D. Larko, Ozone depletion at northern and southern latitudes derived from January 1979 to December 1991 total ozone mapping spectrometer data, *J. Geophys. Res.*, *98*(D7), 12,783-12,793, 1993.

Labitzke, K., and H. van Loon, A note on the distribution of trends below 10 hPa: The extratropical northern hemisphere *Meteorol. Soc. Jpn*, *73*, 883-889, 1995.

London, J., R. D. Bojkov, S. Oltmans, and J. I. Kelley, Atlas of the global distribution of total ozone, July 1957-June 1967, *NCAR Techn. Note 113+STR*, Natl. Center for Atmos. Res., Boulder, Colo., 1976.

Pawson, S., K. Labitzke, R. Lenshow, B. Naujokat, B. Rajiwski, M. Wiesner, and R.-C. Wohlfahrt, *Climatology of the Northern Hemisphere Stratosphere Derived Fom Berlin Analyses*, part 1, *Monthly Means*, 299 pp., Verlag von Dietrich Reimer, Berlin, 1993.

Perlwitz, J., and H.-F. Graf, On the statistical connection between tropospheric and stratospheric circulation of the northern hemisphere in winter, *J. Clim.*, *8*, 2281-2295, 1995.

Perlwitz, J., H.-F. Graf, and I. Kirchner, Increasing greenhouse effect and ozone trends, in *Stratospheric Processes and Their Role in Climate (SPARC)*, Proceedings of the First SPARC General Assembly, Melbourne, Australia, Dec. 1996, WCRP-99, WMO/TD-No. 814, 461-464, 1997

Peters, D., and G. Entzian, January ozone anomaly over the North Atlantic-European region: Longitude-dependent decadal change in total ozone during 1979-1992, *Meteorol Z.*, N. F. 5, 41-44, 1996.

Ramaswamy, V., M. D. Schwarzkopf, and W. J. Randel, Fingerprint of ozone depletion in the spatial and temporal pattern of recent lower-stratospheric cooling, *Nature*, *382*, 616-618, 1996.

Roeckner, E., et al., Simulation of the present-day climate with the ECHAM model: Impact of model physics and resolution, *MPI Rep. 93*, 172 pp , Max-Planck-Inst. für Meteorol., Hamburg, Germany, 1992.

Santer, B. D., et al., A search for human influences on the thermal structure of the atmosphere, *Nature*, *382*, 39-42, 1996.

Stenchikov, G L., I Kirchner, A. Robock, H.-F. Graf, J. C. Antuna, R. Grainger, A. Lambert, and L. Thomason, Radiative forcing from the 1991 Mount Pinatubo volcanic eruption, *MPI Rep. 231*, Max-Planck-Inst. für Meteorol., Hamburg, Germany, Feb. 1997

Stendel, M., and L. Bengtsson, Monitoring the temperature of the troposphere by means of a general circulation model, *MPI-Rep 186*, Max-Planck-Inst. für Meteorol , Hamburg, Germany, Jan 1996.

Wilcox, R W and A. D Belmont, Ozone concentration by latitude, altitude and month, near 80°W. *report*, contract DOT-FA77WA-3999, *Control Data Corp* , Washington, D. C , 1977.

Zhao, X., R. P. Turco, C.-Y. Jim Kao, and S. Elliott, Numerical simulation of the dynamical response of the Arctic vortex to aerosol-associated chemical perturbations in the lower stratosphere, Geophys. *Res Lett.*, *23*, 1525-1528, 1996.

H.-F. Graf, I. Kirchner, J. Perlwitz, Max Planck Institute for Meteorology, Bundesstrasse 55, 20146 Hamburg, Germany. (e-mail: graf@dkrz.de; kirchner@dkrz.de, judith perlwitz@dkrz.de)

(Received April 16, 1997; revised August 22, 1997;
accepted January 27, 1998.)